A zebrafish embryo model for assessment of drug efficacy on mycobacterial persisters

Susanna Commandeur [a,#], Nino Iakobachvili [b,*], Marion Sparrius [a], Mariam Mohamed Nur [b], Galina V. Mukamolova [b] and Wilbert Bitter [a]

Affiliations

[a] Department of Medical Microbiology and Infection Control, Amsterdam UMC, location VUmc, Amsterdam, the Netherlands

[b] Leicester Tuberculosis Research Group, Department of Respiratory Sciences, University of Leicester, Leicester, LE2 9HN, UK

Running title: *M. marinum RpfAB* mutant tolerant to drug *in vivo*

Corresponding author: Susanna Commandeur, s.commandeur@amsterdamumc.nl

* *Present address:* Nino Iakobachvili, The Breast Cancer Now Toby Robins Breast Cancer Research Centre, The Institute of Cancer Research, London, SW3 6JB, UK

Abstract

Tuberculosis continues to kill millions of people each year. The main difficulty in eradication of the disease is the prolonged duration of treatment, which takes at least 6 months. Persister cells have been long associated with failed treatment and disease relapse because of their phenotypical, though transient, tolerance to drugs. By targeting these persisters, the duration of treatment could be shortened, leading to improved tuberculosis treatment and a reduction in transmission. The unique *in vivo* environment drives generation of persisters, however appropriate *in vivo* mycobacterial persister models enabling optimized drug screening are lacking. To set up a persister infection model that is suitable for this, we infected zebrafish embryos with *in vitro* starved *Mycobacterium marinum*. *In vitro* starvation resulted in a persister-like phenotype with the accumulation of stored neutral lipids and concomitant increased tolerance to ethambutol. However, these starved wild-type *M. marinum* rapidly lost their persister phenotype *in vivo.* To prolong the persister phenotype *in vivo* we subsequently generated and analyzed mutants lacking functional resuscitation-promoting factors (Rpfs). Interestingly, the Δ*rpfAB* mutant, lacking two Rpfs, established an infection *in vivo*, whereas a nutrient-starved Δ*rpfAB* mutant did maintain its persister phenotype *in vivo*. This mutant was, after nutrient starvation, also tolerant to ethambutol treatment *in vivo,* as would be expected for persisters. We propose that this zebrafish embryo model with *ΔrpfAB* mutant bacteria is a valuable addition for drug screening purposes and specifically screens to target mycobacterial persisters.

Introduction

Tuberculosis (TB), caused by the bacterium *Mycobacterium tuberculosis*, still results in more than a million deaths each year (1). According to the WHO the TB burden falls too slow in order to reach the milestones set for 2020 by the End TB strategy (1). New approaches should be developed to accelerate the reduction of TB. Standard TB treatment takes at least 6 months. Compliance to the therapy is of tremendous importance for complete elimination of infection, but is challenging for patients because of this long treatment period. Therefore, reducing the time of treatment can contribute to antibiotic compliance, prevention of multi-drug resistance and in the overall reduction of the global TB burden.

It is believed that the prolonged treatment is required because of the presence of so-called *M. tuberculosis* persister cells. These persisters are phenotypically and transiently tolerant to antimicrobials that are used for TB treatment and therefore not efficiently eradicated with a shorter treatment regimen. Although the physiology and regulation of persisters are not fully understood, specific characteristics are linked to the persister state, including the lack of replication, increased tolerance to antimicrobials, altered transcriptional response (2) and the intracellular accumulation of neutral lipids in the form of so-called lipid bodies (3). Different classes of persisters can be discriminated based on their induction, they are either the result of stochastic events or can be generated in response to certain metabolic conditions (2, 4, 5). Persisters are believed to have reduced metabolic activity and the ability to withstand antimicrobial treatment, however establishment of persister genes responsible for these phenotypes has proven to be challenging. This results in ongoing discussions on the uniformity of these persisters and in their classification (6). For instance, some persisters are not able to grow in standard culture media (7, 8). These persisters are dependent on extracellular stimuli that triggers resuscitation. Such triggers include resuscitation-promoting

factors (Rpfs) that are expressed by different mycobacteria (9) and/or peptidoglycan fragments (10). Importantly, mycobacterial persisters that are dependent on Rpfs for resuscitation are produced in high abundance during TB infection (8, 11, 12) and are indeed more tolerant to drugs (13). They were also identified in fish (14) and mice (15, 16) and linked to TB relapse (17). It has been proposed that the unique *in vivo* environment drives *M. tuberculosis* heterogeneity and generation of Rpf-dependent persisters (16).

Compounds that target persisters efficiently will reduce the time of treatment and thus aid in reducing TB burden. To screen for such compounds, models for generation of *M. tuberculosis* persisters are required. Persisters can be induced upon exposure to environmental stresses, of which hypoxia, starvation and low pH are known conditions that *M. tuberculosis* encounters during infection and induces persisters (2). Bacteria can be exposed to such conditions *in vitro*, but compounds should preferably be screened in a host environment and therefore requires a host organism. A highly dynamic environment is present within the host, resulting in heterogeneity within the adapting bacteria (15). Formed persisters are able to withstand the environmental stresses in the host, which are difficult to mimic *in vitro*.

A major challenge in discovery of novel compounds that target persisters is the lack of appropriate in *vivo* models (2, 18). Most *in vivo* mycobacterial work is performed in mice. The Cornell model is a classic system to study persistence of *M. tuberculosis*. Mice are infected with *M. tuberculosis* followed by antimicrobial treatment (isoniazid and pyrazinamide) resulting in complete loss of actively growing bacteria, suggesting clearance of infection. However, after cessation of treatment, active infections develop, indicating the presence of persisters in the treated mice (19). Such a model is suitable for determining the bactericidal effect of compounds that target persisters. Indeed, Hu *et al.* showed that replacing ethambutol for bedaquiline in the standard treatment regimen (rifampicin, isoniazid, pyrazinamide and ethambutol) eliminated the Rpf-dependent *M. tuberculosis* and shortened

treatment time (20). However, (high-throughput) screening of compound libraries is not feasible in such mouse assays and similar issues arise for other *M. tuberculosis* infection models, *e.g.* guinea pigs, rabbits and non-human primates (21, 22).

The zebrafish embryo infection model does allow high-throughput screening (23-25). These zebrafish are infected with the model organism *Mycobacterium marinum,* the causative agent of fish tuberculosis (26). Such an infection results in active disease, showing outgrowth of the bacteria and development of key features of TB, including granuloma formation (26). However, for compound screening we should have a persister population in zebrafish embryos that can be targeted in an *in vivo* setting. To accomplish this, we examined whether the persister state can be established *in vitro*, followed by infection of the embryo with these persisters. In this study we set up an *in vitro* stress condition generating persistent-like *M. marinum*. Stressed wild-type *M. marinum* was still able to regain growth *in vivo* and therefore we generated *rpf* deletion mutants, which should maintain its persister phenotype *in vivo*. Both growth and drug susceptibility of these strains were monitored *in vivo*.

Results

1. Prolonged survival of starved *M. marinum*

M. tuberculosis is able to survive and adapt under different stress conditions. Two most well-studied conditions are hypoxia and starvation. Exposing *M. tuberculosis* to nutrient starvation in PBS supplemented with 0.025% Tween80 induced drug tolerance to TB antimicrobials (27). This phenotype strongly resembles characteristics of persister cells and therefore we hypothesized that exposure of *M. marinum* to this condition could induce *M. marinum* persisters *in vitro*. *M. marinum* is usually grown in nutrient-rich 7H9 medium supplemented with ADC and 0.05% Tween80, which obviously results in increase of both absorbance and CFU number. When *M. marinum* was transferred to PBS with 0.025% Tween80 (starvation condition) growth was halted and there was no increase in CFU counts **(Figure 1)**; nevertheless, the CFU count of these starved *M. marinum* did remain stable over the period of 14 days, indicating that this condition induced a non-growing persister phenotype.

2. Starved *M. marinum* is drug-tolerant and accumulates neutral lipids

Persisters are associated with increased drug tolerance. To test this, the susceptibility of 7H9 and starvation-exposed *M. marinum* to a classical set of TB antimicrobials was determined. Previously, we and others have shown that *M. marinum* has intrinsic resistance to isoniazid and therefore this antimicrobial was not included in this analysis (28-31). The minimal bactericidal concentrations (MBC) of ciprofloxacin, ethambutol, rifampicin and streptomycin were determined for 6 days and 14 days starved *M. marinum* as well as for *M. marinum* grown in nutrient-rich medium (7H9). The cultures were treated for 7 days with a range of antimicrobial concentrations while continuing starvation exposure, after which the bacteria

were plated on agar and CFU counted. The following MBC values were observed for nutrient-rich cultured *M. marinum;* ciprofloxacin (range 4.68-9.3 µg/mL), ethambutol (range 2.34-4.68 µg/mL), rifampicin (1.17 µg/mL) and streptomycin (range 4.68-9.3 µg/mL) **(Figure 2)**. Starved *M. marinum* did not induce tolerance to ciprofloxacin and rifampicin for both 6- and 14-day exposure, as MBC were similar to those of mid-log grown *M. marinum*. Significant tolerance to streptomycin could not be observed after either 6 or 14 days of starvation (4.68 µg/mL and range 9.3-18.75 µg/mL, respectively). However, after 6 days of exposure, the MBC of starved *M. marinum* increased to 18.75 µg/mL (p=0.0043) and after 14 days reached 50 µg/mL (range 37.5-56.25 µg/mL p=0.0281). Thus, exposing *M. marinum* to nutrient starvation induces drug tolerance to ethambutol.

M. tuberculosis use exogenous lipids and store these as triacylglycerol (TAG) in intracellular translucent lipid bodies under non-replicating conditions (32, 33). Since *M. marinum* can use Tween80 as carbon source for growth, probably by releasing the fatty acids of this detergent (34), we determined the capacity of *M. marinum* to accumulate neutral lipid upon nutrient stress exposure, using the neutral lipid dye LD540. *M. marinum* incubated in nutrient-rich 7H9 does not reveal prominent lipid bodies after staining with LD540 **(Figure 3A and B).** However, starvation of *M. marinum* leads to more confined membranes and LD540 positive lipid bodies (**Figure 3C and D**). This could be validated by quantification of LD540 as median fluorescence intensity by flow cytometry (**Figure 3E**). Thus, starvation of *M. marinum* results in accumulation of neutral lipids, thereby replicating another phenotype of *M. tuberculosis* persister cells.

3. ***Persister phenotype of starved*** **M. marinum** ***is not maintained*** **in vivo**

Nutrient-rich cultured *M. marinum* replicates well in zebrafish embryos, establishing an active infection (26) and therefore not suitable for screening compounds that target persisters. Now we had identified a condition that induced a persister-like phenotype we could check how these cells would behave during infection in our zebrafish embryos to generate a persister infection model. 66 and 236 CFU of a 6-day starved *M. marinum* culture was injected in the caudal vein of dechorionated embryos at one day post fertilization (dpf). At 5 days post infection (dpi), embryos were collected and plated on agar to determine the bacterial load per embryo using CFU counts. Although a persister phenotype was observed *in vitro*, starved *M. marinum* rapidly started to grow out in zebrafish embryos in levels comparable to the nutrient-rich grown *M. marinum* **(Supplementary Figure 1)**. This indicates that the persister phenotype of starved *M. marinum* is not maintained in zebrafish embryos and quickly reverted back into the replicative state.

4. Persister phenotype of Δ*rpfAB mutant is maintained* in vivo

Although starved wild-type *M. marinum* is not useful for establishing a persister zebrafish embryo infection model, we reasoned that elimination of reactivation factors could maintain a persister phenotype *in vivo*. For this we focused on the so-called resuscitation promoting factors (Rpfs). Mycobacteria produce multiple Rpf homologues and their expression is tightly regulated (35). In previous research it was shown that *M. marinum* isolated from infected adult zebrafish were able to resuscitate using Rpf, indicating that *M. marinum* could enter a persister state in adult zebrafish and that this population was responsive to Rpfs (14). We hypothesized that by deletion of *rpf* genes, the bacteria will not be able to grow out *in vivo*. The *M. marinum* genome encodes four different *rpf*-like genes, *rpfA, rpfB, rpfC* and *rpfE*. The following single and double mutants were generated in *M. marinum*; Δ*rpfA,* Δ *rpfB* and

188 *ΔrpfAB.* During plating on 7H10 agar we noticed a delay in growth of Δ*rpfAB* mutant as
189 compared to wild-type cells, single mutants and the *ΔrpfAB::B* complemented strain
190 **(Supplementary Figure 2)**. This phenotype was described before in an *ΔrpfACBE* and
191 *ΔrpfACB* mutant of *M. tuberculosis* (36). Though the double Δ*rpfAB* mutant was able to grow
192 comparable to the single mutants and wild-type in nutrient-rich liquid medium
193 **(Supplementary Figure 3A and 3B)**. All strains showed an increase in CFU, followed by a
194 stationary phase in which no loss of CFU could be detected, thus maintained viability.
195 Differences in OD_{600} values can be attributed to clumping of cells. No increase in optical
196 density and CFU could be observed when the mutants were exposed to starvation conditions
197 **(Supplementary Figure 3C and 3D)**. Importantly, Δ*rpfA*, Δ*rpfB* and Δ*rpfAB* mutants
198 remained viable during the 14 days tested, similar to wild-type *M. marinum*.
199 As mentioned previously, starved wild-type *M. marinum* was able to regain growth after
200 zebrafish embryo infection and therefore lost its persister phenotype. To determine whether
201 deletion of *rpf* genes prevent this outgrowth, zebrafish embryos were infected with Δ*rpfA,*
202 Δ*rpfB* and Δ*rpfAB* mutants, either grown in nutrient-rich conditions or exposed to starvation
203 conditions for 6 days. No difference could be observed between the nutrient-rich and nutrient-
204 starved conditions for the single mutants *ΔrpfA* and *ΔrpfB* **(Figure 4)**. Both strains showed
205 further outgrowth after transfer to zebrafish embryos. The nutrient-rich cultured Δ*rpfAB*
206 mutant was also able to establish a full infection in the embryos, comparable to Δ*rpfA* and
207 Δ*rpfB* mutants. However, in contrast, the starved Δ*rpfAB* mutant could not regain growth as
208 its nutrient-rich counterpart, indicating maintenance of the persister phenotype *in vivo*. This
209 lack of regrowth was significantly different as compared to both of the single mutants
210 ($p<0.0001$, **Figure 4**). Furthermore, growth was also restored significantly when *rpfB* was
211 introduced to complement the Δ*rpfAB* mutant ($p=0.014$, **Figure 4**).
212

5. Δ*rpfAB* mutant shows no differences in membrane permeability

The observed loss of growth of this mutant *in vivo* could be due to cell envelope changes and subsequent increased vulnerability to immune factors under starvation conditions. To evaluate the activity and membrane permeability of the wild-type and Δ*rpfAB* mutant a viability stain was performed. Previous work described a method using calcein as cell activity marker (by measuring esterase activity) and the impermeable dye SYTOX green, as membrane permeability marker to determine viability states of *M. tuberculosis* during antibiotic treatment (37). A similar approach was performed by us, using calcein-AM and propidium iodide (PI) staining. Wild-type *M. marinum* grown under nutrient-rich conditions stains positive for calcein (median fluorescence intensity (MFI) of 485), without any PI positive cells, indicating viable cells with intact membranes **(Figure 5A and Supplementary Figure 4).** This phenotype is lost after heat treatment, as observed by a decrease of calcein staining (MFI of 108) and increase in PI staining **(Figure 5B)**. Starvation of *M. marinum* reduces the calcein positivity by half, showing loss of activity (MFI of 207). However, no PI positive cells could be detected which indicates that membranes remain intact during starvation and this phenotype is maintained at day 6 **(Figure 5C and D)**. The nutrient-rich cultured Δ*rpfAB* mutant also showed cell activity as measured by calcein **(Figure 5E)**, although having higher fluorescent intensity (MFI of 1612) when compared to wild-type. Nevertheless, a loss of calcein fluorescence is observed when exposed to starvation conditions (MFI of 525) **(Figure 5F)**, which is also maintained after 6 days of starvation **(Figure 5G).** Importantly, no increase in PI positive cells is observed, indicating that both starved wild-type and Δ*rpfAB* bacteria reduce cell activity while maintaining intact membranes.

When membranes become more permeable, more dye can pass and bind to the DNA, this was previously shown for ethidium bromide dye, e.g. (34), and more recently shown for DAPI

(38). Heat-killed bacteria stained brighter for Syto62, but this was not observed for starved wild-type and Δ*rpfAB* mutant, indicating again that membrane integrity was not compromised by starvation **(Supplementary Figure 5)**.

Lastly, we also tested the effect of chemicals used for embryo homogenization on *M. marinum* viability. Nutrient-rich and nutrient-starved wild-type and Δ*rpfAB* mutant were exposed to mycoprep buffer, mycoprep, SDS and mycoprep with SDS for 10 minutes, followed by CFU plating. No difference between wild-type and Δ*rpfAB* mutant was observed and therefore this cannot explain the loss of growth observed in the zebrafish embryos (data not shown).

6. Starved *ΔrpfAB* mutant is tolerant to ethambutol *in vivo*

Since the starved Δ*rpfAB* mutant maintains its persister phenotype *in vivo*, we hypothesized that it could also remain tolerant to ethambutol under these conditions. Therefore, we infected zebrafish embryos with either nutrient-rich or nutrient-starved wild-type and Δ*rpfAB* mutant. After 1 day of infection ethambutol was added to the water in two doses (40 µg/mL and 80 µg/mL). Five days after infection the bacterial load was determined by measuring fluorescent pixels per embryo. A significant decrease in bacterial load was observed for nutrient-rich and nutrient-starved wild-type *M. marinum* when treated with 40 and 80 µg/mL ethambutol **(Figure 6A**). This further validates the loss of its persistent phenotype *in vivo* for the nutrient-starved wild type bacteria. A significant decrease of bacterial load was also observed for nutrient-rich cultured Δ*rpfAB* mutant after treatment with either 40 µg/mL or 80 µg/mL of ethambutol. However, in line with our previous finding no drop in bacterial load could be detected for starved Δ*rpfAB* **(Figure 6B),** indicating that starved Δ*rpfAB* becomes tolerant to ethambutol in zebrafish embryos. Introduction of *rpfB* to the double mutant partly restored the

wild-type phenotype; starved Δ*rpfAB::rpfB* treated with 80 µg/mL of ethambutol showed a significant drop in bacterial load **(Figure 6C)**. Microscopy images show that infection with starved wild-type *M. marinum* results in bacterial spread throughout the zebrafish embryo and development of early granulomas **(Supplementary Figure 6A), as previously reported** (24). In contrast, limited spread could be observed upon starved Δ*rpfAB* infection, bacterial fluorescence localized mostly to the caudal vein but was also observed at the spinal cord. Though clustering of bacteria could be observed, which could indicate initiation of granuloma formation **(Supplementary Figure 6B)**. Overall, this confirms indeed that starved Δ*rpfAB* is able to maintain the persister phenotype *in vivo* during the timeframe used for these experiments.

Discussion

Multiple approaches have been described for generating mycobacteria with a persister phenotype *in vitro (2).* Our goal was to identify a model that is as reproducible as possible and controlled efficiently. Nutrient starvation was most appropriate for our experiments with *M. marinum*. It is hypothesized that nutrient deprivation occurs in host environments like phagocytes and in the granuloma (39). In 1933, Loebel *et al.* studied the effect of starvation and added 'foodstuffs' on survival of *M. tuberculosis* and discovered that *M. tuberculosis* remains viable after prolonged (55 days) incubation in a solution of saline and phosphate, which was due to reduced oxygen consumption (40). Bacilli that were starved in distilled water were viable even after 2 years of storage (41). Betts et al. later showed that exposure of *M. tuberculosis* to PBS revealed downregulation of genes involved in, among others, energy metabolism and translation, indicating adaptation to starvation stress, but also induced drug tolerance (42).

Gengenbacher et al. reproduced the work of Loebel and Betts and further validated that drug tolerance was induced in starved persister cultures (27). Starving *M. tuberculosis* in PBS containing Tween80 0.025% for 14 days resulted in induced tolerance to rifampicin, streptomycin, moxifloxacin and isoniazid (27), but also to fluoroquinolones, rifamycins and ethambutol (43). Additional transcriptomic analysis confirmed distinct gene expression patterns in starved *M. tuberculosis* (44) Therefore, we continued to study the effect of *M. marinum* under this specific nutrient stress.

Our work revealed an increased tolerance of starved *M. marinum* to ethambutol. Gengenbacher et al. explained this increased tolerance by a reduced uptake of antimicrobials, though this was not the case for ethambutol (43). Ethambutol targets the cell wall by inhibiting the biosynthesis of arabinogalactan and arabinomannan. More specifically,

ethambutol targets arabinosyl transferases encoded by the *embCAB* operon (45-47). Both EmbA and EmbB are required for arabinogalactan synthesis and EmbC plays a role in arabinomannan synthesis (48). All three proteins encoded by the *embCAB* operon are predicted integral membrane proteins with multiple transmembrane domains and suggested to be localized in the cytoplasmic membrane and protein function suggested to be performed in the periplasmic space (48). Three mechanisms could affect ethambutol activity and could explain the difference in MBC observed for nutrient-rich and starved *M. marinum*; (i) First, since starved *M. tuberculosis* and *M. marinum* stop dividing, probably no or limited new cell wall is formed and therefore inhibition by ethambutol has no effect, (ii) second, arabinogalactan could be not essential for starved bacteria or lastly, (iii) the detergent effect of Tween80 might wane over time, resulting in restoration of the capsule leading to decreased permeability (49).

No statistical difference in MBC was observed for the other tested antimicrobials. Ciprofloxacin inhibits DNA gyrase, preventing the unwinding of DNA. Rifampicin inhibits RNA polymerase, preventing RNA synthesis. Both antimicrobials prevent transcription and our results indicate that transcription is still essential for starved *M. marinum* up to day 14. The same holds true for streptomycin, which targets protein translation. These results indicate that ciprofloxacin, rifampicin and streptomycin are still able to enter the cell. These three antimicrobials were not tested by Gengenbacher, but related fluoroquinolones and rifamycins showed, in contrast to our data, less intracellular accumulation (43).

Besides induced tolerance to ethambutol, *M. marinum* was non-dividing and viable and accumulated neutral lipids and therefore this starved condition induced persister-like *M. marinum*. Though *in vitro* models only mimic assumed environmental conditions, such as hypoxia, acidic environment and starvation of different nutrients, either in single or combined setting, all having their identified tolerance to antimicrobials (2). These conditions however

do not completely mimic the complexity present *in vivo*. One major drawback is the variation in treatment success between *in vitro* and *in vivo* as discussed by Gold *et al.* (2). Metronidazole, an antimicrobial targeting anaerobic bacteria, works well on hypoxic *M. tuberculosis* cultures, but lacks activity in different animal models and humans (2). Therefore *in vivo* models are still essential.

Zebrafish embryo infection with nutrient-rich cultured *M. marinum* results in outgrowth of the bacteria, establishing an active infection ((26), this study), and therefore does not develop a prominent persister population for drug screening purposes. However, a prolonged infection results in arise of an Rpf-dependent population (14); thus, persisters can be formed in zebrafish. Though such a prolonged infection results in loss of high-throughput capacity and thus zebrafish embryo infection requires *in vitro* cultured persister cells. To test whether our persister-like starved *M. marinum* would remain in a persistent state *in vivo*, zebrafish embryos were infected with these cells. Although we managed to generate a persister-like phenotype in *M. marinum in vitro*, these persisters regained full potential to replicate in the zebrafish embryos. Upon caudal vein infection, bacteria first enter the blood stream and will be rapidly taken up by macrophages. These cells will form the center of the early granulomas after traversing endothelial and epithelial barriers (26). This first contact to the embryo host environment most likely contains more nutrients compared to the starvation condition *in vitro*, resulting in regained growth. In order to prevent this loss of persister phenotype, we tested the ability of starved *rpf* mutants to regain growth in zebrafish embryos.

Single *M. tuberculosis rpf* mutants do not show defects in *in vitro* and *in vivo* growth (50, 51). We also observed that single Δ*rpfA* and Δ*rpfB* mutants are still able to regain growth in zebrafish embryos, even after *in vitro* starvation, which is in agreement with the dispensability of the *M. tuberculosis rpfA* and *rpfB* genes *in vivo* (50). However, upon exposure of the *ΔrpfAB M. marinum* mutant to starvation conditions a persister phase is generated that is

maintained during zebrafish embryo infection. This approach prevented the reactivation that was observed for wild-type and single mutants. Thus, despite exposure to a novel environmental condition, *ΔrpfAB* is unable to completely revert back to growing conditions in the tested timeframe.

M. tuberculosis single *rpf* mutants do not have an *in vivo* growth defect, but *M. tuberculosis* Δ*rpfB* mutant does have a delayed reactivation in chronic *M. tuberculosis* infected mice treated with aminoguanidine (52). A later study showed an even stronger delay in reactivation for an Δ*rpfAB* double mutant using the same reactivation model or other reactivation model (53). In addition, a delay in growth and generation of a chronic infection prior reactivation treatment was observed (53). This indicates that the *M. tuberculosis* Δ*rpfAB* mutant entered the persister phase *in vivo* and therefore is unable to revert back to active growth conditions. In our hands Δ*rpfA, ΔrpfB and Δrpf*AB *M marinum* mutants were able to establish a comparable *M. marinum* infection, indicating that the bacteria in zebrafish embryos do not enter a persister phase. Persisters are most likely not formed within the short time frame used for our embryo infection model, as discussed previously (24, 26), whereas this does occur within the longer time frame used for mice. But nevertheless, both RpfA and RpfB proteins seem to be important for reactivation (53).

We also noticed a growth delay of Δ*rpfAB* mutant on plate after inoculation from -80 ºC stock. A similar delay was described for *M. tuberculosis* Δ*rpfACBE* and Δ*rpfACBED* mutants (36), which the authors attributed to cell wall defects, making them vulnerable for immediate stress conditions on the plate. Interestingly, similar results are described for mutations of both *rpf* genes from *Listeria monocytogenes* (54). The growth delay we observed for *M. marinum* Δ*rpfAB,* could not attributed to a general cell wall defect. Instead we expect that the observed delay occurs because of prior exposure to -80 ºC stress, which fits with the lack of outgrowth in zebrafish embryos when prior exposed to starvation.

We observed an increased calcein fluorescence in Δ*rpfAB* mutant. Calcein-AM is not fluorescent and membrane permeable. Upon intracellular esterase hydrolysis, liberated fluorescent calcein becomes membrane impermeable and remains in the cell. One explanation could be that calcein is more actively exported via membrane pumps in wild-type *M. marinum*, a mechanism also described for eukaryotic cells (55).

Since we were now able to keep a persister form in the embryo infection model, we could also test the antimicrobial tolerance *in vivo*. Kana *et al*. showed previously that targeting *M. tuberculosis* Δ*rpfAB in vitro* with different drugs, including ethambutol, revealed MIC profiles comparable to the wild-type strain, indicating no increased susceptibility to TB drugs (56). Previously, ethambutol treatment of an active *M. marinum* infection in adult zebrafish resulted in a significant reduction of the bacterial load, whereas the bacterial load in a latent infection was not reduced with this antimicrobial (28). Ethambutol reduced the bacterial load of wild-type *M. marinum*, either cultured under nutrient-rich or starved conditions. However, we could not completely clear the infection as DsRed2 fluorescence was still detected. The presence of stochastic persisters might be the cause of this observation. Although most of the bacteria actively divide and spread, a minority of bacteria may have a persister phenotype (57). This also explains the biphasic killing curve often observed (e.g. (57, 58)). Furthermore, drug tolerance in *M. marinum* is induced within days in individual macrophages after infection of zebrafish embryos (59). These factors may contribute to the lack of complete clearance in our model. Nevertheless, we showed in this work that the starved *ΔrpfAB* was also not killed by ethambutol *in vivo*, but the nutrient-rich cultured *ΔrpfAB* was. With this data we can further validate that the persister phase generated by nutrient starvation *in vitro* is maintained. Here we showed that we were able to generate a persister infection model in zebrafish embryos, using starved *ΔrpfAB M. marinum* cells. The lack of both *rpfA* and *rpfB* prevented the reactivation of *M. marinum* in our zebrafish embryo model. This state made *M.*

marinum unresponsive to ethambutol *in vivo.* Although this model is suitable for high-throughput screening, follow-up studies on potential hits need to be performed to assess e.g. activity against *M. tuberculosis* and pharmacodynamics.

Thus, *in vitro* studies using environmental stress conditions to induce persisters provide promising compounds that target persisters (2, 60). Though these need to be validated in *in vivo* models. Direct screening of compounds targeting persisters within an *in vivo* model would greatly improve detection of potential hits. As we are dealing with a lack of appropriate *in vivo* models for persister drug screening, we want to propose this model for the search of novel compounds that specifically target mycobacterial persisters.

Materials and methods

Bacterial strains

Wild-type *M. marinum* M (61) and mutant strains were grown in 7H9 (Difco) liquid medium supplemented with Middlebrook albumin, dextrose and catalase (ADC, BD Biosciences) and 0.05% (w/v) Tween80 at 30 ºC under shaking conditions (90 rpm) or maintained on 7H10 (Difco) agar plates supplemented with Middlebrook oleic acid, albumin, dextrose and catalase (OADC, BD biosciences) at 30 ºC. Kanamycin (25 µg/mL) or hygromycin (50 µg/mL) was added when required.

Starvation of bacterial cultures

Wild-type and mutant strains were grown in 7H9 to mid-log phase. Bacteria were collected, centrifuged (16.000 x*g*) and supernatant removed. Pellet was resuspended in PBS supplemented with 0.025% Tween80 (Merck) OD_{600} adjusted to 0.2-0.3 OD_{600}/mL and incubated at 30 ºC under shaking conditions (90 rpm).

Antimicrobial susceptibility assay

Ciprofloxacin (Fluka), ethambutol (Sigma), rifampicin (Sigma) and streptomycin (Sigma) were diluted to 300 µg/mL in PBS containing Tween80 0.025% and dispensed in 2-fold dilution in a 96-well plate format. Starved and log-culture bacteria (1*10^4 per well diluted in PBS tween80 0.025%) were inoculated in the plates, in the presence of a 2-fold dilution series in PBS Tween80 0.025%. Plates were incubated for 1 week followed by resuspension of wells and plating 5 µL on 7H10 agar to determine the minimal bactericidal concentration (MBC).

Neutral lipid analysis

Nutrient-rich or starved culture (adjusted to OD 0.25-0.5) were pelleted by centrifugation at 16.000 x*g*. Pellet was resuspended in 4% paraformaldehyde (Sigma), incubated for 30 minutes and washed by PBS. Bacteria were stained with neutral lipid dye LD540 (1 µg/mL, kindly provided by prof. Thiele, Bönn, Germany (62)) for 30 minutes in the dark on ice. PBS was added and centrifuged. For flow cytometry, stained cells were filtered over a 50 µM mesh filter (Vlint) and acquired on an Attune NxT flow cytometer (Thermofisher) equipped with a 488 nm laser to excite LD540.

Rpf mutants

In-frame unmarked *rpf* deletion mutants were generated using homologous recombination approach as described by Parish et al (63). Briefly, 1.5 kb flanking regions (FR1 And FR2) of *rpfA* (mmar_4665) and *rpfB* (mmar_4479) were amplified from *M. marinum* genome using Platinum Taq polymerase (Invitrogen) and corresponding primers (**Table S1**). Fragments were cloned in p2NIL plasmid, followed by cloning of a marker cassette from pGOAL19 plasmid in PacI site. All fragments were sequenced by GATC.

Electrocompetent *M. marinum* cells were prepared by washing cells from a mid-logarithmic phase culture (OD_{600} ~06-0.8) with 10% (v/v) sterile glycerol three times at room temperature. DNA (3 µg) was dissolved in 3 µL of DNAse/RNAse free sterile water and mixed with 400 µL of electrocompetent cells. The cells containing DNA were transferred to a 2 mm long-electrode electroporation cuvette (Protech International). An electroporation pulse was delivered at 2500 V, 1000 Ω and 25 µF. The electroporated cells were mixed with 7H9 medium and incubated overnight at 32 °C without shaking. Single crossover colonies were selected on 7H10 agar containing kanamycin (50 µg/mL) and 5-bromo-4-chloro-3-indolyl β-D-galactopyranoside (50 µg/mL). Single crossover cells were grown in 7H9 medium and double crossovers selected by plating on 7H10 agar containing 2 % (w/v) sucrose. Deletion

462 mutants were confirmed by PCR using relevant test primers (**Table S1**), southern
463 hybridization and sequencing.
464 For complementation of Δ*rpfAB* mutant with *rpfB* gene, a 200 bp-upstream region was cloned
465 into the pMV306 that integrates at *attB* site of *M. marinum* chromosome. For visualization of
466 *M. marinum* in zebrafish embryos, a plasmid expressing dsRed2 under control of the PSM12
467 promoter (Plasmid #30171, kindly provided by Dr. Monica Hagedorn, University of Geneva,
468 Switzerland) was electroporated in all strains.
469
470 *Zebrafish embryo infection*
471 Prior infection, *M. marinum* was incubated in PBS tween80 0.025% for 6 days and control
472 conditions were grown in 7H9 to mid-log phase. Cultures were harvested and pellet
473 resuspended in 0.2% phenol red (Sigma). Adult transparent *casper* zebrafish (64) were
474 maintained in aerated 5 liter tanks and held at 26 °C. A 14:10 h light-dark cycle was used.
475 Eggs were harvested within 2 hours after fertilization, sorted in E3 medium supplemented
476 with methylene blue (0.3 mg/mL) and incubated o/n at 30 °C. One dpf embryos were
477 mechanically dechorionated and infected with *M. marinum* by injection in the caudal vein as
478 previously described (65). After infection, embryos were kept in chorion water at 28 °C for 5
479 days. When required, ethambutol was added to the chorion water at 1 day post infection
480 (dpi). At 5 dpi, embryos were dissociated in 5% SDS (Sigma) and subsequently Mycoprep
481 (BD biosciences) was added and incubated for 10 minutes followed by addition of PBS and
482 centrifugation. Supernatant was plated to determine the bacterial load per embryo.
483 Alternatively, bacterial fluorescence was measured per embryo using Olympus IX83
484 fluorescent microscope equipped with Orca-flash 4.0 LT camera. Brightfield and fluorescent
485 images were analyzed using CellProfiler 3.15. Previously we have shown that CFU ratios
486 between conditions are highly comparable to the ratios obtained by fluorescence analysis (24),

making fluorescent analysis a reliable method for quantification of the bacterial load in embryos. Embryos were anesthetized in chorion medium supplemented with 0.02% MS-222 prior injection and dissociation.

Ethics statement

All procedures involving zebrafish were carried out in accordance with appropriate guidelines and regulations. Breeding of adult fish was approved by the local animal welfare committee (Animal Experimental licensing Committee, DEC) of the Amsterdam UMC location VU University Medical Center and held according standard protocols (zfin.org). Procedures involving zebrafish embryos all complied to the international guidelines specified by the EU Animal Protection Directive, which allows the use of zebrafish up to the free-living stage and was also approved by DEC Amsterdam UMC location VU University Medical Center.

Flow cytometry analysis of viable cells

Nutrient-rich and starved cultures were harvested at different timepoints. Bacteria were stained with Propidium Iodide (PI, 40 µg/ml, Thermofisher), Calcein-AM (1:200, Thermofisher) and Syto62 (1:1000, Thermofisher) in 7H9 at 30 ˚C for 30 minutes. After staining the bacteria were washed, filtered over a 50 µM mesh filter and acquired on an NxT flow cytometer (Thermofisher) equipped with 488 nm, 561 nm and 638 lasers used to excite calcein, PI and Syto62, respectively. Unstained and fluorescence minus one (FMO) controls were included. Single bacteria were gated (66) and a minimum of 20.000 events was acquired for each sample. Syto62 was used as a marker for bacterial events. Acquired data was compensated and analyzed using FCSExpress version 7.

Acknowledgements

This study was funded by the Innovative Medicines Initiative Joint Undertaking under grant agreement 115337, the resources of which are composed of financial contribution from the European Union's Seventh Framework Programme (FP7/2007-2013) and EFPIA companies' in-kind contribution (W. Bitter); a VENI grant (016.Veni.171.088) from the Netherlands Organization for Scientific Research (NWO) (S. Commandeur) and UK Biotechnology and Biological Sciences Research Council through a Doctoral Training Programme award (NI) and a grant BB/K000330/1 (G.V. Mukamolova). The authors acknowledge Coen Kuijl and Lynn Mes for technical assistance and are grateful to Hajra Okhai, Janie Liaw and Fareed Alrekani for help with cloning and screening of *rpf* mutants.

The authors declare no financial or personal conflict of interest.

References

1. WHO. 2018. Global Tuberculosis Report 2018 World Health Organization, Geneva
2. Gold B, Nathan C. 2017. Targeting Phenotypically Tolerant Mycobacterium tuberculosis. Microbiol Spectr 5.
3. Maurya RK, Bharti S, Krishnan MY. 2018. Triacylglycerols: Fuelling the Hibernating Mycobacterium tuberculosis. Front Cell Infect Microbiol 8:450.
4. Harms A, Maisonneuve E, Gerdes K. 2016. Mechanisms of bacterial persistence during stress and antibiotic exposure. Science 354.
5. Ehrt S, Schnappinger D, Rhee KY. 2018. Metabolic principles of persistence and pathogenicity in Mycobacterium tuberculosis. Nat Rev Microbiol 16:496-507.
6. Lipworth S, Hammond RJ, Baron VO, Hu Y, Coates A, Gillespie SH. 2016. Defining dormancy in mycobacterial disease. Tuberculosis (Edinb) 99:131-42.
7. Mukamolova GV, Kaprelyants AS, Kell DB, Young M. 2003. Adoption of the transiently non-culturable state--a bacterial survival strategy? Adv Microb Physiol 47:65-129.
8. Chengalroyen MD, Beukes GM, Gordhan BG, Streicher EM, Churchyard G, Hafner R, Warren R, Otwombe K, Martinson N, Kana BD. 2016. Detection and Quantification of Differentially Culturable Tubercle Bacteria in Sputum from Patients with Tuberculosis. Am J Respir Crit Care Med 194:1532-1540.
9. Kana BD, Mizrahi V. 2010. Resuscitation-promoting factors as lytic enzymes for bacterial growth and signaling. FEMS Immunol Med Microbiol 58:39-50.
10. Nikitushkin VD, Demina GR, Shleeva MO, Kaprelyants AS. 2013. Peptidoglycan fragments stimulate resuscitation of "non-culturable" mycobacteria. Antonie Van Leeuwenhoek 103:37-46.

11. Mukamolova GV, Turapov O, Malkin J, Woltmann G, Barer MR. 2010. Resuscitation-promoting factors reveal an occult population of tubercle Bacilli in Sputum. Am J Respir Crit Care Med 181:174-80.
12. Rosser A, Stover C, Pareek M, Mukamolova GV. 2017. Resuscitation-promoting factors are important determinants of the pathophysiology in Mycobacterium tuberculosis infection. Crit Rev Microbiol 43:621-630.
13. Turapov O, O'Connor BD, Sarybaeva AA, Williams C, Patel H, Kadyrov AS, Sarybaev AS, Woltmann G, Barer MR, Mukamolova GV. 2016. Phenotypically Adapted Mycobacterium tuberculosis Populations from Sputum Are Tolerant to First-Line Drugs. Antimicrob Agents Chemother 60:2476-83.
14. Parikka M, Hammaren MM, Harjula SK, Halfpenny NJ, Oksanen KE, Lahtinen MJ, Pajula ET, Iivanainen A, Pesu M, Ramet M. 2012. Mycobacterium marinum causes a latent infection that can be reactivated by gamma irradiation in adult zebrafish. PLoS Pathog 8:e1002944.
15. Dhar N, McKinney J, Manina G. 2016. Phenotypic Heterogeneity in Mycobacterium tuberculosis. Microbiol Spectr 4.
16. Turapov O, Glenn S, Kana B, Makarov V, Andrew PW, Mukamolova GV. 2014. The in vivo environment accelerates generation of resuscitation-promoting factor-dependent mycobacteria. Am J Respir Crit Care Med 190:1455-7.
17. Hu Y, Liu A, Ortega-Muro F, Alameda-Martin L, Mitchison D, Coates A. 2015. High-dose rifampicin kills persisters, shortens treatment duration, and reduces relapse rate in vitro and in vivo. Front Microbiol 6:641.
18. Zhang Y, Yew WW, Barer MR. 2012. Targeting persisters for tuberculosis control. Antimicrob Agents Chemother 56:2223-30.

19. Scanga CA, Mohan VP, Joseph H, Yu K, Chan J, Flynn JL. 1999. Reactivation of latent tuberculosis: variations on the Cornell murine model. Infect Immun 67:4531-8.
20. Hu Y, Pertinez H, Liu Y, Davies G, Coates A. 2019. Bedaquiline kills persistent Mycobacterium tuberculosis with no disease relapse: an in vivo model of a potential cure. J Antimicrob Chemother 74:1627-1633.
21. Alnimr AM. 2015. Dormancy models for Mycobacterium tuberculosis: A minireview. Braz J Microbiol 46:641-7.
22. Patel K, Jhamb SS, Singh PP. 2011. Models of latent tuberculosis: their salient features, limitations, and development. J Lab Physicians 3:75-9.
23. Ordas A, Raterink RJ, Cunningham F, Jansen HJ, Wiweger MI, Jong-Raadsen S, Bos S, Bates RH, Barros D, Meijer AH, Vreeken RJ, Ballell-Pages L, Dirks RP, Hankemeier T, Spaink HP. 2015. Testing tuberculosis drug efficacy in a zebrafish high-throughput translational medicine screen. Antimicrob Agents Chemother 59:753-62.
24. Stoop EJ, Schipper T, Rosendahl Huber SK, Nezhinsky AE, Verbeek FJ, Gurcha SS, Besra GS, Vandenbroucke-Grauls CM, Bitter W, van der Sar AM. 2011. Zebrafish embryo screen for mycobacterial genes involved in the initiation of granuloma formation reveals a newly identified ESX-1 component. Dis Model Mech 4:526-36.
25. Veneman WJ, Marin-Juez R, de Sonneville J, Ordas A, Jong-Raadsen S, Meijer AH, Spaink HP. 2014. Establishment and optimization of a high throughput setup to study Staphylococcus epidermidis and Mycobacterium marinum infection as a model for drug discovery. J Vis Exp doi:10.3791/51649:e51649.
26. van Leeuwen LM, van der Sar AM, Bitter W. 2014. Animal models of tuberculosis: zebrafish. Cold Spring Harb Perspect Med 5:a018580.

27. Gengenbacher M, Rao SP, Pethe K, Dick T. 2010. Nutrient-starved, non-replicating Mycobacterium tuberculosis requires respiration, ATP synthase and isocitrate lyase for maintenance of ATP homeostasis and viability. Microbiology 156:81-7.
28. Myllymaki H, Niskanen M, Luukinen H, Parikka M, Ramet M. 2018. Identification of protective postexposure mycobacterial vaccine antigens using an immunosuppression-based reactivation model in the zebrafish. Dis Model Mech 11.
29. Aubry A, Jarlier V, Escolano S, Truffot-Pernot C, Cambau E. 2000. Antibiotic susceptibility pattern of Mycobacterium marinum. Antimicrob Agents Chemother 44:3133-6.
30. Li G, Lian LL, Wan L, Zhang J, Zhao X, Jiang Y, Zhao LL, Liu H, Wan K. 2013. Antimicrobial susceptibility of standard strains of nontuberculous mycobacteria by microplate Alamar Blue assay. PLoS One 8:e84065.
31. Boot M, Sparrius M, Jim KK, Commandeur S, Speer A, van de Weerd R, Bitter W. 2016. iniBAC induction Is Vitamin B12- and MutAB-dependent in Mycobacterium marinum. J Biol Chem 291:19800-12.
32. Daniel J, Maamar H, Deb C, Sirakova TD, Kolattukudy PE. 2011. Mycobacterium tuberculosis uses host triacylglycerol to accumulate lipid droplets and acquires a dormancy-like phenotype in lipid-loaded macrophages. PLoS Pathog 7:e1002093.
33. Barisch C, Soldati T. 2017. Mycobacterium marinum Degrades Both Triacylglycerols and Phospholipids from Its Dictyostelium Host to Synthesise Its Own Triacylglycerols and Generate Lipid Inclusions. PLoS Pathog 13:e1006095.
34. Ates LS, Ummels R, Commandeur S, van de Weerd R, Sparrius M, Weerdenburg E, Alber M, Kalscheuer R, Piersma SR, Abdallah AM, Abd El Ghany M, Abdel-Haleem AM, Pain A, Jimenez CR, Bitter W, Houben EN. 2015. Essential Role of the ESX-5

623 Secretion System in Outer Membrane Permeability of Pathogenic Mycobacteria. PLoS
624 Genet 11:e1005190.
625 35. Schwenk S, Arnvig KB. 2018. Regulatory RNA in Mycobacterium tuberculosis, back
626 to basics. Pathog Dis 76.
627 36. Kana BD, Gordhan BG, Downing KJ, Sung N, Vostroktunova G, Machowski EE,
628 Tsenova L, Young M, Kaprelyants A, Kaplan G, Mizrahi V. 2008. The resuscitation-
629 promoting factors of Mycobacterium tuberculosis are required for virulence and
630 resuscitation from dormancy but are collectively dispensable for growth in vitro. Mol
631 Microbiol 67:672-84.
632 37. Hendon-Dunn CL, Doris KS, Thomas SR, Allnutt JC, Marriott AA, Hatch KA,
633 Watson RJ, Bottley G, Marsh PD, Taylor SC, Bacon J. 2016. A Flow Cytometry
634 Method for Rapidly Assessing Mycobacterium tuberculosis Responses to Antibiotics
635 with Different Modes of Action. Antimicrob Agents Chemother 60:3869-83.
636 38. Ekiert DC, Bhabha G, Isom GL, Greenan G, Ovchinnikov S, Henderson IR, Cox JS,
637 Vale RD. 2017. Architectures of Lipid Transport Systems for the Bacterial Outer
638 Membrane. Cell 169:273-285 e17.
639 39. Berney M, Berney-Meyer L. 2017. Mycobacterium tuberculosis in the Face of Host-
640 Imposed Nutrient Limitation. Microbiol Spectr 5.
641 40. Loebel RO, Shorr E, Richardson HB. 1933. The Influence of Adverse Conditions
642 upon the Respiratory Metabolism and Growth of Human Tubercle Bacilli. J Bacteriol
643 26:167-200.
644 41. Nyka W. 1974. Studies on the effect of starvation on mycobacteria. Infect Immun
645 9:843-50.

646 42. Betts JC, Lukey PT, Robb LC, McAdam RA, Duncan K. 2002. Evaluation of a
647 nutrient starvation model of Mycobacterium tuberculosis persistence by gene and
648 protein expression profiling. Mol Microbiol 43:717-31.
649 43. Sarathy J, Dartois V, Dick T, Gengenbacher M. 2013. Reduced drug uptake in
650 phenotypically resistant nutrient-starved nonreplicating Mycobacterium tuberculosis.
651 Antimicrob Agents Chemother 57:1648-53.
652 44. Cortes T, Schubert OT, Rose G, Arnvig KB, Comas I, Aebersold R, Young DB. 2013.
653 Genome-wide mapping of transcriptional start sites defines an extensive leaderless
654 transcriptome in Mycobacterium tuberculosis. Cell Rep 5:1121-31.
655 45. Goude R, Amin AG, Chatterjee D, Parish T. 2009. The arabinosyltransferase EmbC is
656 inhibited by ethambutol in Mycobacterium tuberculosis. Antimicrob Agents
657 Chemother 53:4138-46.
658 46. Belanger AE, Besra GS, Ford ME, Mikusova K, Belisle JT, Brennan PJ, Inamine JM.
659 1996. The embAB genes of Mycobacterium avium encode an arabinosyl transferase
660 involved in cell wall arabinan biosynthesis that is the target for the antimycobacterial
661 drug ethambutol. Proc Natl Acad Sci U S A 93:11919-24.
662 47. Telenti A, Philipp WJ, Sreevatsan S, Bernasconi C, Stockbauer KE, Wieles B, Musser
663 JM, Jacobs WR, Jr. 1997. The emb operon, a gene cluster of Mycobacterium
664 tuberculosis involved in resistance to ethambutol. Nat Med 3:567-70.
665 48. Abrahams KA, Besra GS. 2018. Mycobacterial cell wall biosynthesis: a multifaceted
666 antibiotic target. Parasitology 145:116-133.
667 49. Sani M, Houben EN, Geurtsen J, Pierson J, de Punder K, van Zon M, Wever B,
668 Piersma SR, Jimenez CR, Daffe M, Appelmelk BJ, Bitter W, van der Wel N, Peters
669 PJ. 2010. Direct visualization by cryo-EM of the mycobacterial capsular layer: a labile
670 structure containing ESX-1-secreted proteins. PLoS Pathog 6:e1000794.

50. Tufariello JM, Jacobs WR, Jr., Chan J. 2004. Individual Mycobacterium tuberculosis resuscitation-promoting factor homologues are dispensable for growth in vitro and in vivo. Infect Immun 72:515-26.
51. Downing KJ, Betts JC, Young DI, McAdam RA, Kelly F, Young M, Mizrahi V. 2004. Global expression profiling of strains harbouring null mutations reveals that the five rpf-like genes of Mycobacterium tuberculosis show functional redundancy. Tuberculosis (Edinb) 84:167-79.
52. Tufariello JM, Mi K, Xu J, Manabe YC, Kesavan AK, Drumm J, Tanaka K, Jacobs WR, Jr., Chan J. 2006. Deletion of the Mycobacterium tuberculosis resuscitation-promoting factor Rv1009 gene results in delayed reactivation from chronic tuberculosis. Infect Immun 74:2985-95.
53. Russell-Goldman E, Xu J, Wang X, Chan J, Tufariello JM. 2008. A Mycobacterium tuberculosis Rpf double-knockout strain exhibits profound defects in reactivation from chronic tuberculosis and innate immunity phenotypes. Infect Immun 76:4269-81.
54. Pinto D, Sao-Jose C, Santos MA, Chambel L. 2013. Characterization of two resuscitation promoting factors of Listeria monocytogenes. Microbiology 159:1390-401.
55. Hollo Z, Homolya L, Davis CW, Sarkadi B. 1994. Calcein accumulation as a fluorometric functional assay of the multidrug transporter. Biochim Biophys Acta 1191:384-8.
56. Kana BD, Mizrahi V, Gordhan BG. 2010. Depletion of resuscitation-promoting factors has limited impact on the drug susceptibility of Mycobacterium tuberculosis. J Antimicrob Chemother 65:1583-5.
57. Keren I, Minami S, Rubin E, Lewis K. 2011. Characterization and transcriptome analysis of Mycobacterium tuberculosis persisters. mBio 2:e00100-11.

696 58. Ahmad Z, Klinkenberg LG, Pinn ML, Fraig MM, Peloquin CA, Bishai WR,
697 Nuermberger EL, Grosset JH, Karakousis PC. 2009. Biphasic kill curve of isoniazid
698 reveals the presence of drug-tolerant, not drug-resistant, Mycobacterium tuberculosis
699 in the guinea pig. J Infect Dis 200:1136-43.
700 59. Adams KN, Takaki K, Connolly LE, Wiedenhoft H, Winglee K, Humbert O, Edelstein
701 PH, Cosma CL, Ramakrishnan L. 2011. Drug tolerance in replicating mycobacteria
702 mediated by a macrophage-induced efflux mechanism. Cell 145:39-53.
703 60. Defraine V, Fauvart M, Michiels J. 2018. Fighting bacterial persistence: Current and
704 emerging anti-persister strategies and therapeutics. Drug Resist Updat 38:12-26.
705 61. Ramakrishnan L, Falkow S. 1994. Mycobacterium marinum persists in cultured
706 mammalian cells in a temperature-restricted fashion. Infect Immun 62:3222-9.
707 62. Spandl J, White DJ, Peychl J, Thiele C. 2009. Live cell multicolor imaging of lipid
708 droplets with a new dye, LD540. Traffic 10:1579-84.
709 63. Parish T, Stoker NG. 2000. Use of a flexible cassette method to generate a double
710 unmarked Mycobacterium tuberculosis tlyA plcABC mutant by gene replacement.
711 Microbiology 146 (Pt 8):1969-1975.
712 64. White RM, Sessa A, Burke C, Bowman T, LeBlanc J, Ceol C, Bourque C, Dovey M,
713 Goessling W, Burns CE, Zon LI. 2008. Transparent adult zebrafish as a tool for in
714 vivo transplantation analysis. Cell Stem Cell 2:183-9.
715 65. Benard EL, van der Sar AM, Ellett F, Lieschke GJ, Spaink HP, Meijer AH. 2012.
716 Infection of zebrafish embryos with intracellular bacterial pathogens. J Vis Exp
717 doi:10.3791/3781.
718 66. Ates LS, van der Woude AD, Bestebroer J, van Stempvoort G, Musters RJ, Garcia-
719 Vallejo JJ, Picavet DI, Weerd R, Maletta M, Kuijl CP, van der Wel NN, Bitter W.

2016. The ESX-5 System of Pathogenic Mycobacteria Is Involved In Capsule Integrity and Virulence through Its Substrate PPE10. PLoS Pathog 12:e1005696.

Figure legends

Figure 1. Survival of starved M. marinum

Growth curves of *M. marinum* inoculated in 7H9 or PBS tw80 0.025%. Both optical density (A) and colony forming units (CFU) (B) were determined per mL (n=3). All significant differences are indicated in the graph.

Figure 2. Starvation induces drug tolerance in M. marinum

M. marinum was cultured in nutrient-rich 7H9 medium (light orange bars) or exposed to starvation conditions for 6 days (orange bars) or 14 days (dark orange bars). After incubation cultures were treated with ciprofloxacin, ethambutol, rifampicin or streptomycin for an additional 7 days, followed by plating on 7H10 agar. CFU were allowed to grow and the minimal bactericidal concentration (MBC) was determined based on loss of CFU (n= three biological replicates). Two-way ANOVA using Tukey's multiple comparisons test was used to determine significance. A *p*-value of <0.05 was considered significant. All significant differences are indicated in the graph (* = $p \leq 0.05$, ** = $p \leq 0.01$).

Figure 3. Starved M. marinum *accumulates neutral lipids*

LD540 staining of nutrient-rich 7H9 cultured (A and B) and starvation exposed (4 days) (C and D) *M. marinum*. A and C represents phase contrast images and B and D fluorescent images. LD540 median fluorescence intensity was quantified by flow cytometry (E).

Figure 4. Persister phenotype ΔrpfAB mutant maintained in vivo

One dpf zebrafish embryos were infected with either nutrient-rich *M. marinum* (orange) or 6-day starved *M. marinum* (purple). Infection was maintained for 5 days. Bacterial load (CFU)

was determined per embryo and log-transformed. One-way ANOVA using Tukey's multiple comparisons test was used to determine significance. A *p*-value of <0.05 was considered significant. All significant differences are indicated in the graph (* = $p \leq 0.05$, ** = $p \leq 0.01$, **** = $p \leq 0.0001$). Inoculum of all strains ranged between 11-95 CFU.

Figure 5. Starved wild-type and ΔrpfAB mutant shows reduced cell activity while maintaining membrane integrity

Wild-type (A-D) and *ΔrpfAB* mutant (E-G) strains were either cultured in nutrient-rich (A, E) or starved (C-D and F-G) conditions and after 2 (C, F) and 6 (D, G) days, cells were stained with Syto62, calcein-AM and PI. Fluorescence was assessed by flow cytometry. Acquired data of at least 20.000 events per sample was analyzed as described in Materials and Methods. Data is presented as flow cytometry scatter plots of bacterial events. Calcein-AM positive and PI negative events correspond to viable bacteria. Representative data from two independent experiments is shown.

Figure 6. Starved ΔrpfAB mutant is tolerant to ethambutol in vivo

One dpf embryos were infected with nutrient-rich (red circles) or starved (blue circles) wild-type *M. marinum* (A), *ΔrpfAB* mutant (B) or *ΔrpfAB::B* complemented strain (C). After one day of infection the embryos were treated with ethambutol (40 or 80 µg/mL). Five days after infection bacterial load was determined by measuring DsRed2 fluorescence per embryo using Cellprofiler. Obtained values were log-transformed and significance determined via one-way anova using Tukey's multiple comparisons test. A *p*-value of <0.05 was considered significant. All significant differences are indicated in the graph (* = $p \leq 0.05$, ** = $p \leq 0.01$, *** = $p \leq 0.001$, **** = $p \leq 0.0001$) Two inocula were used per condition and ranged

773 between 9 and 173 CFU. Dotted line indicates the threshold of the assay, indicating no
774 detected fluorescence.

Figure 1

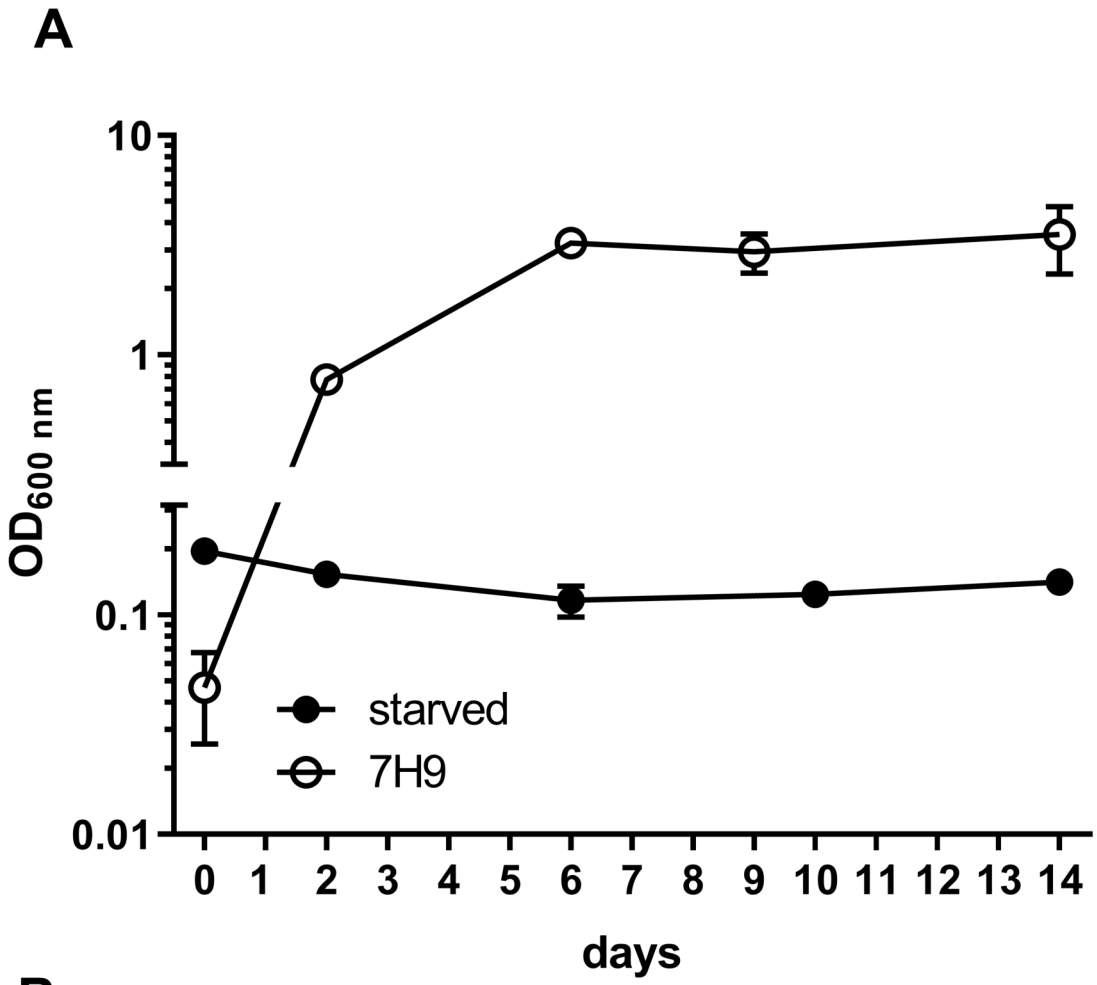
A
10
1
0.1
0.01
$OD_{600\ nm}$
starved
7H9
0 1 2 3 4 5 6 7 8 9 10 11 12 13 14
days

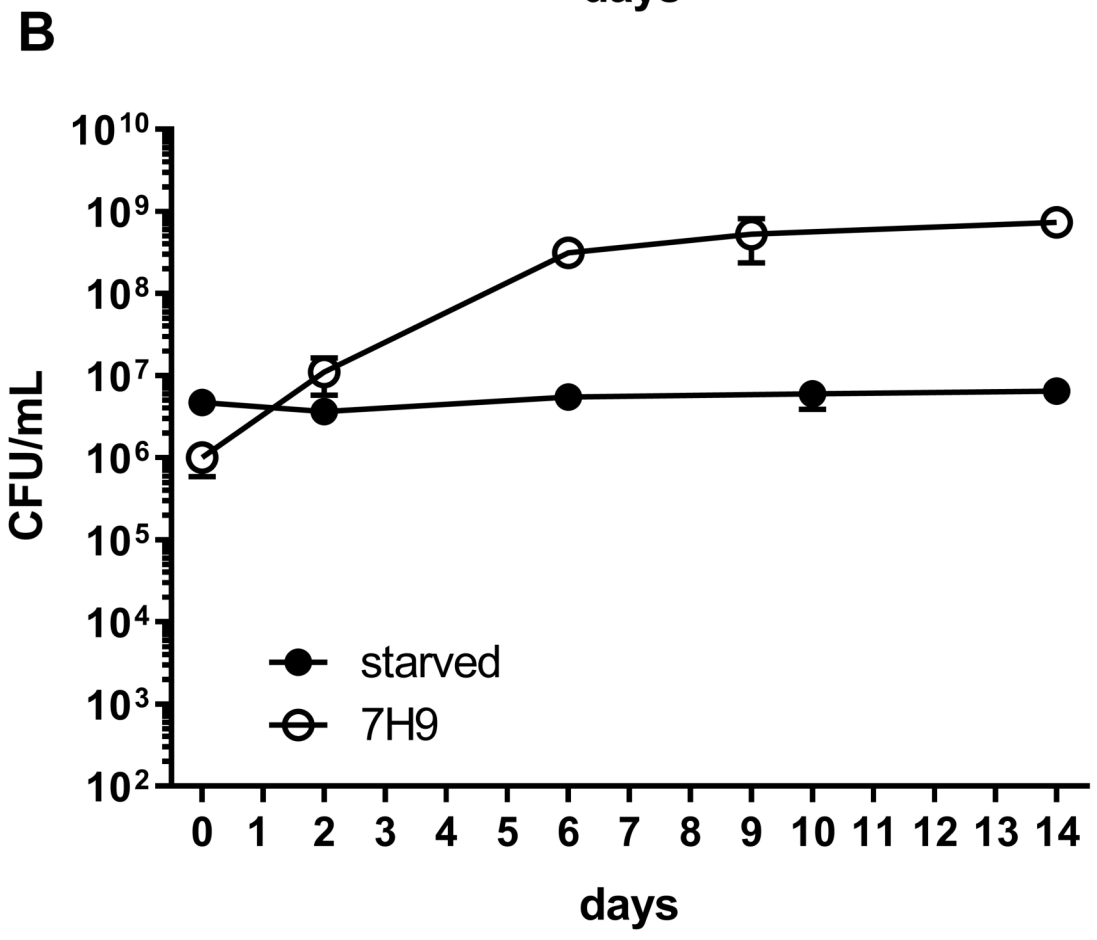
B
10^{10}
10^{9}
10^{8}
10^{7}
10^{6}
10^{5}
10^{4}
10^{3}
10^{2}
CFU/mL
starved
7H9
0 1 2 3 4 5 6 7 8 9 10 11 12 13 14
days

Figure 2

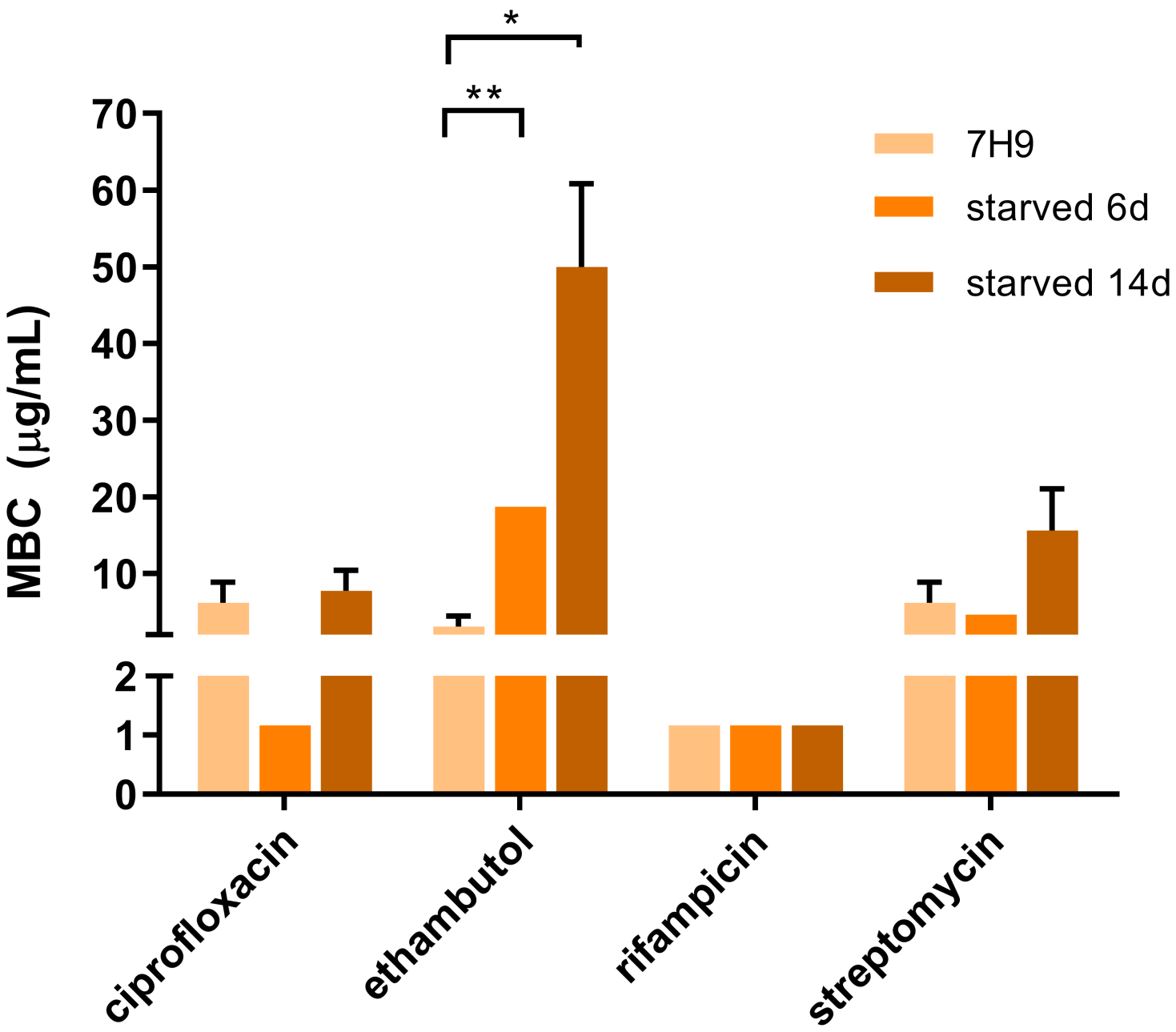
*
**
70
60
50
40
30
20
10
2
1
0
MBC (µg/mL)
7H9
starved 6d
starved 14d
ciprofloxacin
ethambutol
rifampicin
streptomycin

Figure 3

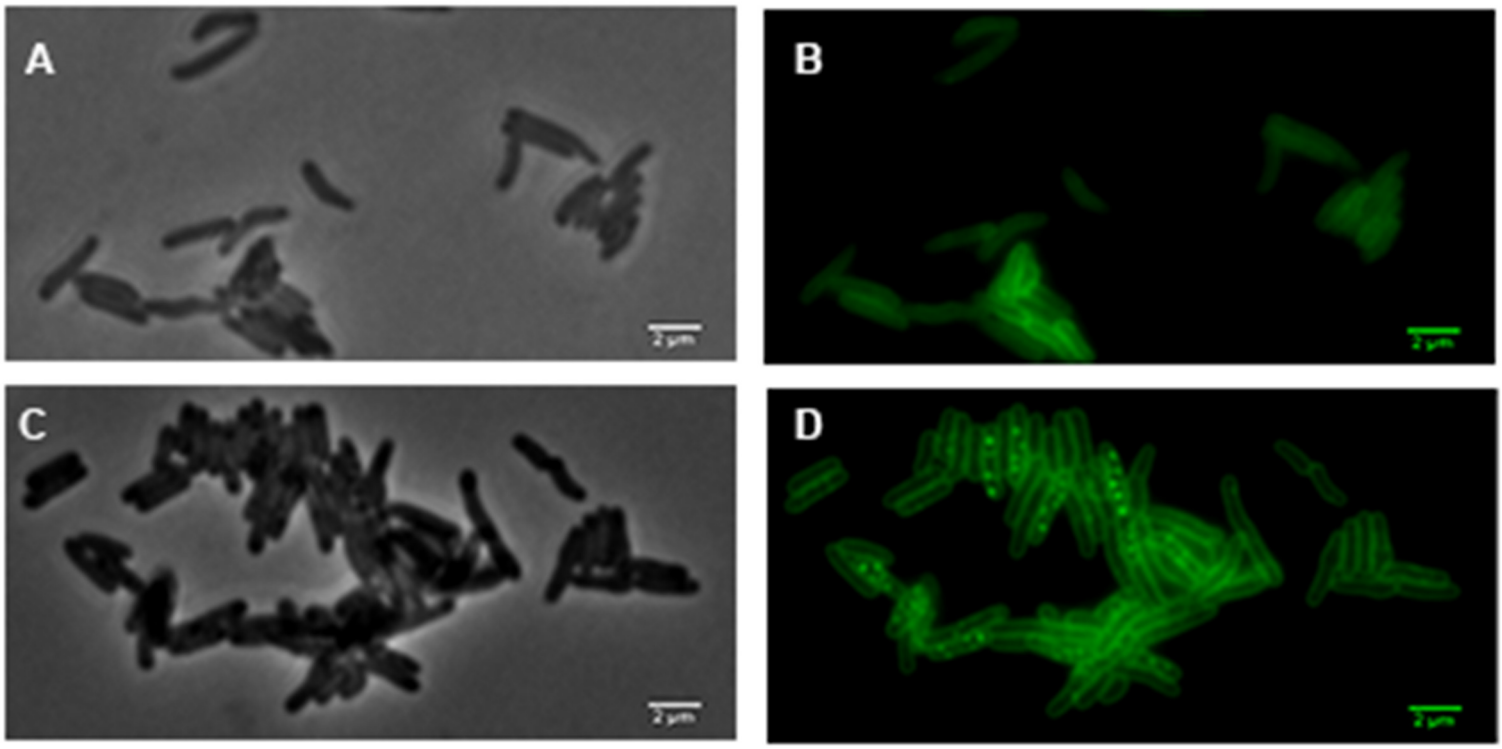
A
B
C
D
2 µm
2 µm
2 µm
2 µm

E

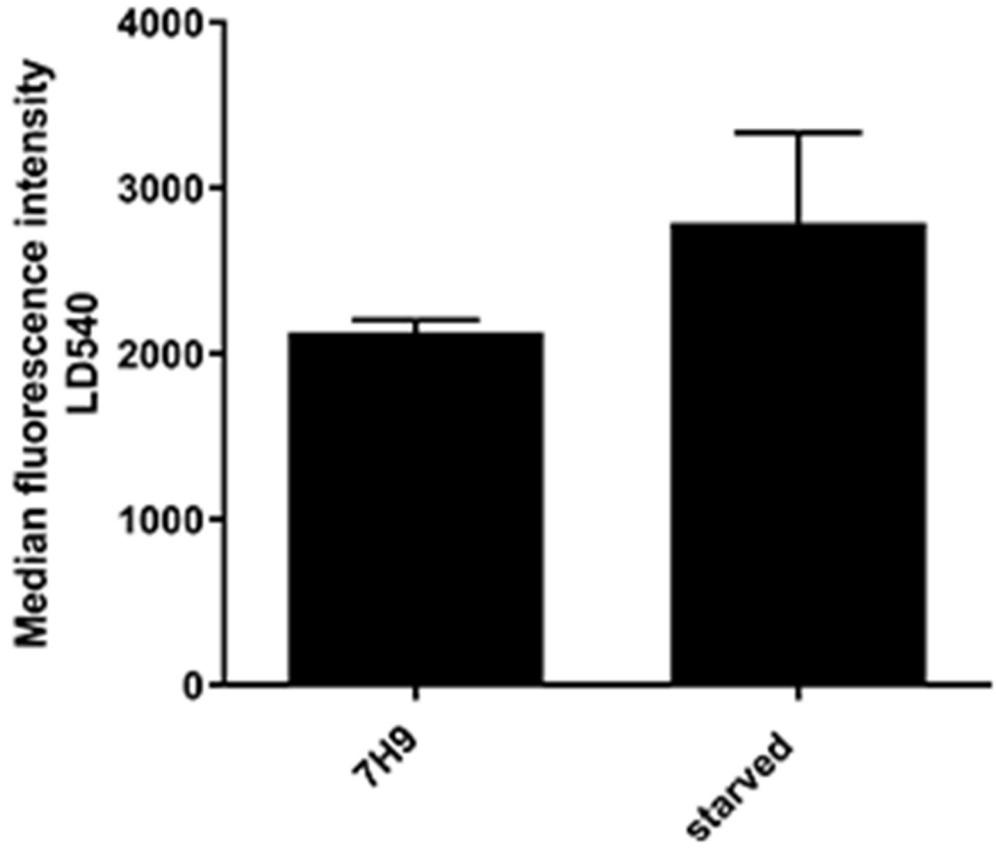
Median fluorescence intensity
LD540
4000
3000
2000
1000
0
7H9
starved

Figure 4

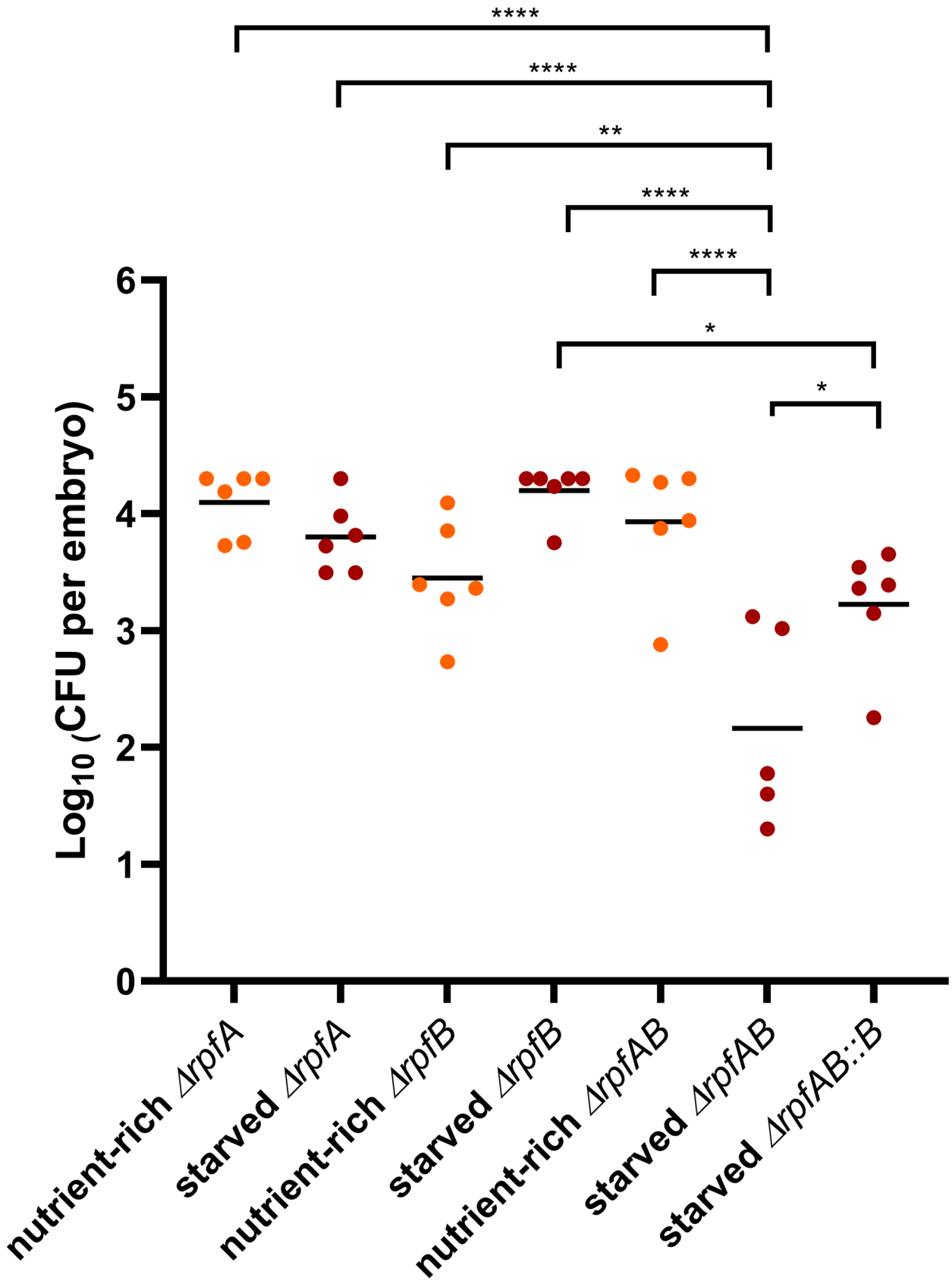
****
****
**
****
****
*
*
6
5
4
3
2
1
0
Log10 (CFU per embryo)
nutrient-rich ΔrpfA
starved ΔrpfA
nutrient-rich ΔrpfB
starved ΔrpfB
nutrient-rich ΔrpfAB
starved ΔrpfAB
starved ΔrpfAB::B

Figure 5

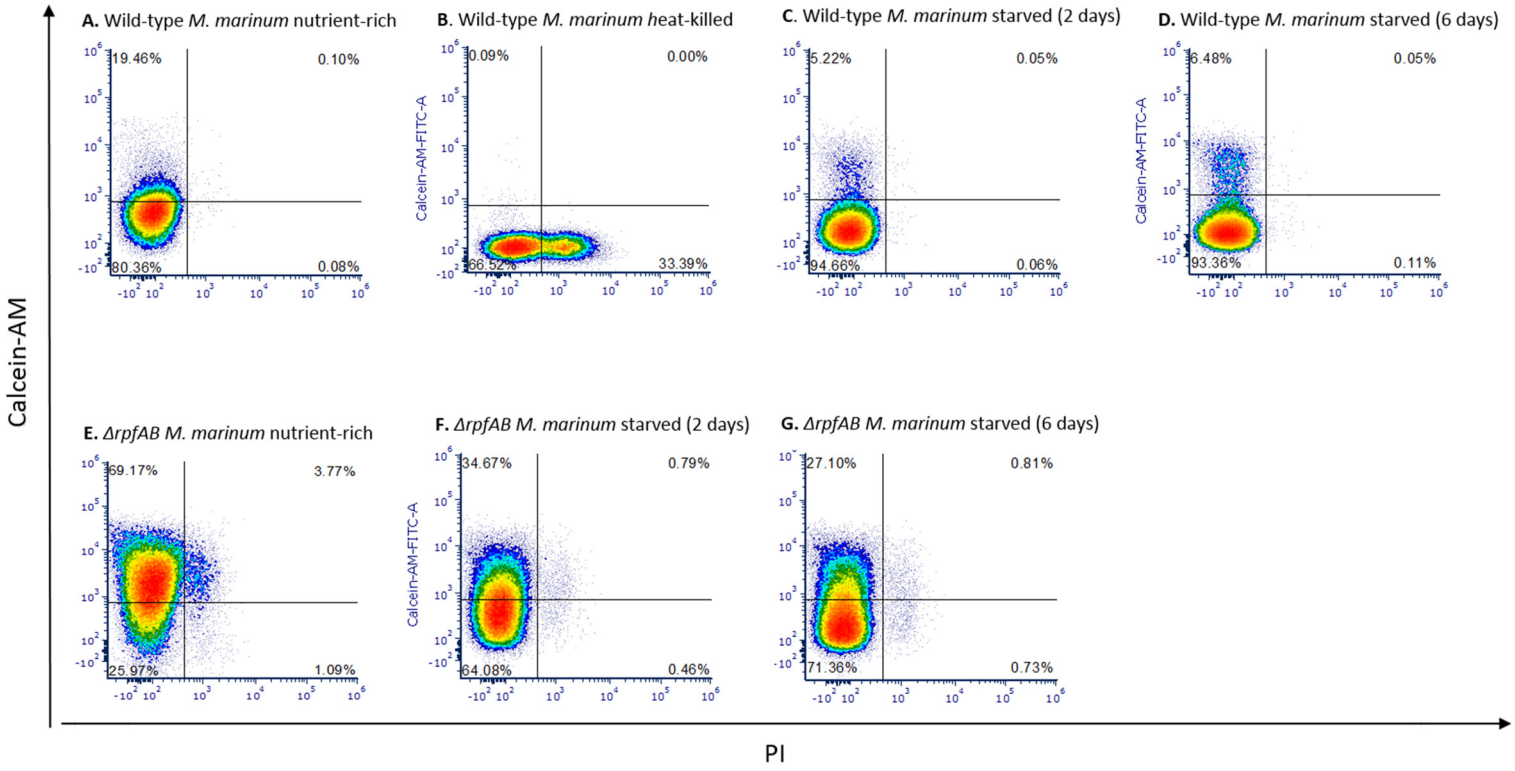
A. Wild-type M. marinum nutrient-rich
19.46%
0.10%
80.36%
0.08%
B. Wild-type M. marinum heat-killed
0.09%
0.00%
66.52%
33.39%
C. Wild-type M. marinum starved (2 days)
5.22%
0.05%
94.66%
0.06%
D. Wild-type M. marinum starved (6 days)
6.48%
0.05%
93.36%
0.11%
E. ΔrpfAB M. marinum nutrient-rich
69.17%
3.77%
25.97%
1.09%
F. ΔrpfAB M. marinum starved (2 days)
34.67%
0.79%
64.08%
0.46%
G. ΔrpfAB M. marinum starved (6 days)
27.10%
0.81%
71.36%
0.73%
Calcein-AM
Calcein-AM-FITC-A
PI

Figure 6

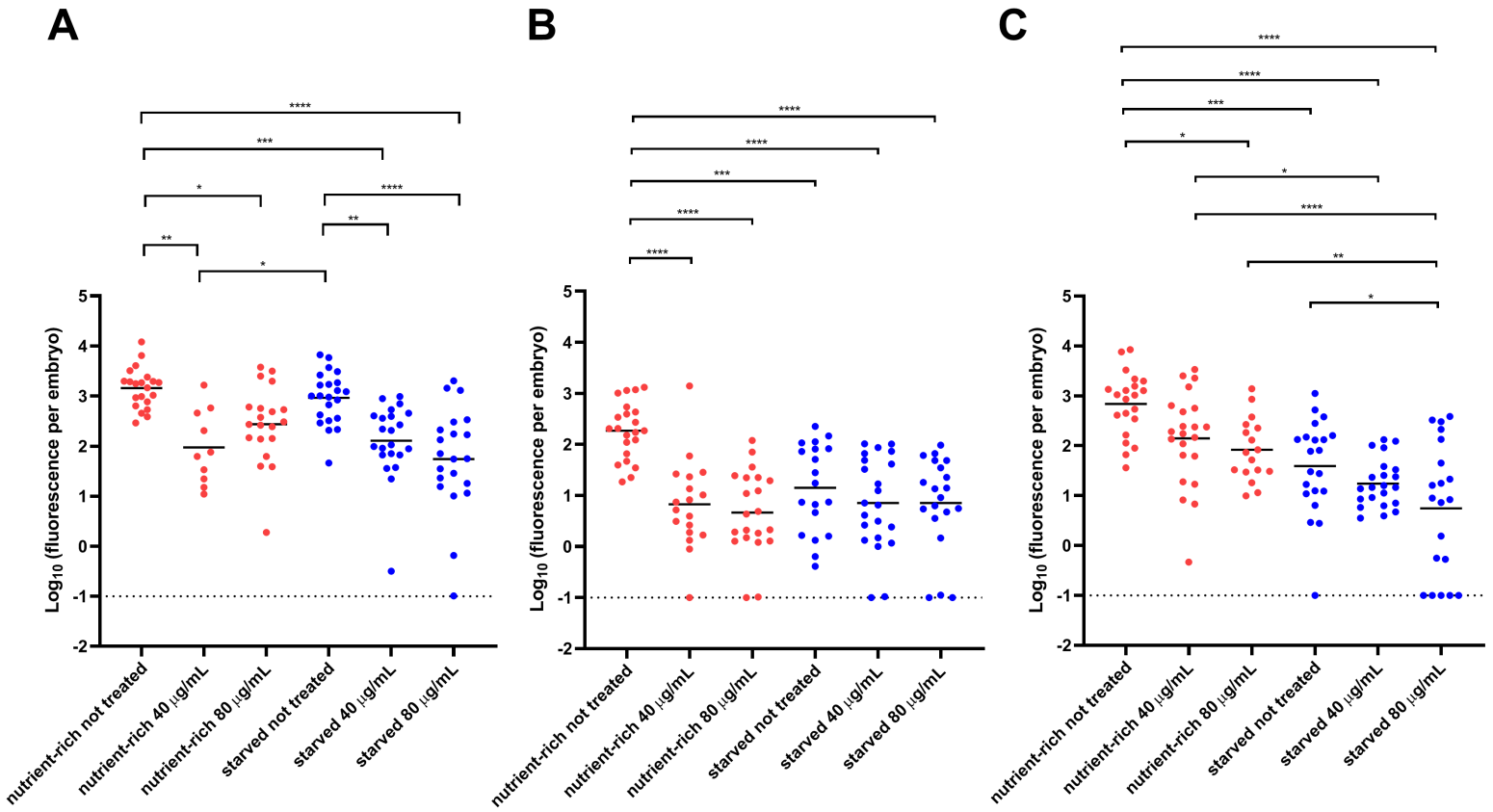
A
B
C
Log10 (fluorescence per embryo)
nutrient-rich not treated
nutrient-rich 40 µg/mL
nutrient-rich 80 µg/mL
starved not treated
starved 40 µg/mL
starved 80 µg/mL